



Independent contributions of tropical sea surface temperature modes to the interannual variability of western North Pacific tropical cyclone frequency

Jinjie Song^{1,2}  | Philip J. Klotzbach³ | Nannan Qin^{1,2}  | Yihong Duan²

¹Nanjing Joint Institute for Atmospheric Sciences, Chinese Academy of Meteorological Sciences, Nanjing, China

²State Key Laboratory of Severe Weather, Chinese Academy of Meteorological Sciences, Beijing, China

³Department of Atmospheric Science, Colorado State University, Fort Collins, Colorado, USA

Correspondence

Jinjie Song, Nanjing Joint Institute for Atmospheric Sciences, Chinese Academy of Meteorological Sciences, 8 Yushun Road, Nanjing 210041, China.
Email: songjinjie@qq.com

Funding information

National Natural Science Foundation of China, Grant/Award Numbers: 41905001, 42175007, 42192552, 42192554, 61827901, U2342203; G. Unger Vetlesen Foundation

Abstract

This study investigates the independent contributions of three tropical sea surface temperature anomaly (SSTA) modes to interannual changes in summertime western North Pacific (WNP) tropical cyclone (TC) frequency from 1982 to 2022. We primarily analyse partial regressions of TC metrics and environmental variables onto the El Niño–Southern Oscillation Modoki (ENM), North Indian Ocean (NIO) SSTA and tropical North Atlantic (TNA) SSTA indices. We find that although basinwide WNP TC frequency significantly correlates with both the ENM and NIO indices, the regions with the most significant changes in TC formation induced by these two indices are well separated. During El Niño Modoki, significant increases in TC formation concentrate over the southeastern part of the WNP, while during a warm NIO, significant decreases in TC formation concentrate over the northwestern part of the WNP. By contrast, insignificant changes in TC genesis over the WNP are solely induced by TNA SSTAs. We show that the two pathways of TNA SSTA's influence on WNP TC activity through modulation of Pacific and NIO SSTAs are of comparable importance. During El Niño Modoki, significantly enhanced TC genesis over the southeastern WNP can be explained by more favourable environmental conditions, which is linked to an anomalous low-level cyclonic circulation over the WNP. During a warm NIO, TC genesis is significantly suppressed over the northwestern WNP, due primarily to an anomalous low-level anticyclonic circulation-induced decrease in relative vorticity. By contrast, during a warm TNA, no notable changes in environmental variables are found over most of the WNP, while significant flow anomalies are limited to the central-to-eastern Pacific and the western Atlantic. These results highlight that the TNA SSTA by itself has a limited impact on WNP TC genesis and the associated large-scale environment.

KEYWORDS

El Niño–Southern Oscillation Modoki, North Indian Ocean, tropical cyclone, tropical North Atlantic, western North Pacific

1 | INTRODUCTION

Tropical cyclones (TCs) are one of the most severe natural disasters around the world, causing considerable social and economic damage due to the accompanying strong winds, heavy rainfall and storm surge. The western North Pacific (WNP) is the most TC-active basin worldwide, accounting for approximately one-third of global TCs on an annually averaged basis (Lee et al., 2012). Given heightened concern about the impact of climate change, increasing attention has been paid to the temporal variability of WNP TC activity as modulated by various climate phenomena (Walsh et al., 2016).

El Niño–Southern Oscillation (ENSO) is a major mode influencing interannual changes in frequency, intensity, formation location and lifespan of WNP TCs (Emanuel, 2018). Traditionally, ENSO has been categorized into two flavours: canonical ENSO (CEN) (also known as conventional ENSO, cold tongue ENSO or eastern Pacific ENSO) and ENSO Modoki (ENM) (also known as warm pool ENSO or central Pacific ENSO), with peak sea surface warming/cooling centred over the eastern equatorial Pacific and the central equatorial Pacific, respectively (Capotondi et al., 2015; Kao & Yu, 2009; Timmermann et al., 2018). CEN does not significantly affect basinwide WNP TC frequency, although it does cause a significant southeast–northwest shift in average WNP TC formation location (e.g., Chan, 1985, 2000; Lander, 1994; Li & Zhou, 2012; Saunders et al., 2000; Wang & Chan, 2002). By contrast, there is a significant interannual relationship between basinwide WNP TC frequency and ENM (e.g., Chen & Tam, 2010; Kim et al., 2011; Li & Wang, 2014; Patricola et al., 2018; Wang et al., 2013; Zhang et al., 2015). During ENM, TC formation is enhanced over most of the WNP, due to a large-scale anomalous cyclonic circulation, anomalous ascending motion, as well as an anomalously moist mid-troposphere. These conditions arise due to the maximum oceanic warming occurring over the central Pacific, as would be expected based on Gill's model (Gill, 1980).

The Pacific meridional mode (PMM) is another climate mode over the tropical Pacific that modulates WNP TC activity. Previous studies (e.g., Fu et al., 2023; Zhang et al., 2016, 2020; Wu et al., 2020) reported a basinwide enhancement (suppression) of TC activity during the positive (negative) phase of the PMM, which was further linked to PMM-induced changes in the large-scale circulation over the WNP. There is also a significant positive relationship between the PMM and the frequency of intense TCs over the WNP as well as landfalling TCs in China (Gao et al., 2018a, 2018b, 2020a, 2020b). Positive phases of the PMM favour an anomalous low-level cyclonic circulation over most of the WNP, favouring

more frequent TC formations over the main development region. These TCs then tend to move westward/northwestward and subsequently make landfall in China (Gao et al., 2018a, 2018b, 2020a, 2020b).

Recently, several studies have reported on a remote modulation of interannual TC frequency over the WNP by sea surface temperature (SST) anomalies (SSTAs) over other tropical ocean basins. There is a significant inverse relationship between basinwide WNP TC frequency and SSTAs over the tropical Indian Ocean (IO) (e.g., Du et al., 2011; Gao et al., 2020a, 2020b; Ha et al., 2015; Zhan et al., 2011a, 2011b, 2014; Zheng et al., 2016). During warm tropical IO years, TC formation is suppressed over most of the WNP, leading to a significant decrease in basinwide TC frequency. This decrease has been mainly linked to a large-scale anomalous low-level anticyclonic circulation over the WNP. Tropical IO warming can excite a warm equatorial Kelvin wave that penetrates eastward into the equatorial western Pacific, inducing surface convergence on the equator and surface divergence off the equator. This subsequently triggers an anomalous WNP anticyclone (Xie et al., 2009, 2016).

There is also a notable negative correlation between basinwide WNP TC frequency and tropical North Atlantic (TNA) SSTAs (e.g., Cao et al., 2016; Gao et al., 2018a, 2018b; Huo et al., 2015; Jin et al., 2022; Yu et al., 2016a). A significant decrease in basinwide WNP TC frequency occurs during warm TNA years, driven by TC-suppressing large-scale conditions over the WNP, including reduced low-level vorticity and mid-level humidity and enhanced vertical wind shear (VWS). As reported in previous publications (e.g., Gao et al., 2018a, 2018b; Huo et al., 2015; Wang, 2019; Yu et al., 2016a), two possible pathways have been suggested for linking SSTAs over the TNA to environmental changes over the WNP. Warm TNA SSTAs can trigger anomalous atmospheric deep convection. This deep convection is associated with eastward-propagating Kelvin waves and westward-propagating Rossby waves. The Kelvin wave-related anomalous easterlies over the North IO (NIO) decelerate the climatological winds, suppressing surface evaporation and thus warming the NIO through a wind–evaporation–SST (WES) feedback (Xie & Philander, 1994). The Rossby wave-related anomalous westerlies over the off-equatorial northeastern Pacific induce local ocean cooling via the WES mechanism. This cooling further propagates equatorward and westward, generating anomalous cooling over the equatorial central Pacific (Xie, 1999). Both pathways indirectly influence changes in WNP environmental conditions by warming the NIO or cooling the equatorial central Pacific.

As summarized in Wang (2019), the Pacific, IO and Atlantic interact significantly with each other. SSTAs in

one basin can induce corresponding SST changes in the other two basins via various atmospheric and oceanic pathways, on timescales ranging from months to decades. It is therefore possible that the impacts of SSTAs over different basins on WNP TC frequency are not independent. Wang and Wang (2019) found that the two leading empirical orthogonal function (EOF) modes of the western Pacific subtropical high could integrate the influences of trans-basin SST anomalies over the Pacific, Atlantic and IO on WNP TC activity. The first mode integrated the effects of ENSO and Atlantic SST anomalies, while the second mode incorporated the effects of SST anomalies over the Indo-Pacific warm pool and IO (Wang & Wang, 2019).

By using an EOF analysis, Yu et al. (2016b) quantitatively analysed the relative contributions of leading SSTA modes in each basin to changes in WNP TC frequency. They found that the first SSTA modes over the Pacific, IO and Atlantic accounted for 0.8%, 17.6% and 14.3% of the total variance of WNP TC frequency changes on inter-annual timescales, respectively. Nonetheless, because the EOF analysis was not performed over the globe, the variances explained by SSTA modes over different basins may overlap.

Given that the ENM and SSTAs over the IO and Atlantic can all lead to basinwide changes in WNP TC formation, we investigate whether their-induced spatial patterns of WNP TC formation changes are similar. In particular, it is still unknown whether there are differences in the significant regions of TC formation changes modulated by SSTAs over different basins. Although the TNA has been shown to influence WNP TC activity by modulating SSTAs over the Pacific (e.g., Huo et al., 2015) and over the IO (e.g., Yu et al., 2016a), it remains unclear as to how TNA SSTAs modulate WNP TC activity via the Pacific and IO SSTA pathways. Furthermore, we quantify the contributions of TNA SSTAs in modulating WNP TC formation through these different pathways.

To answer the above questions, this study focuses on analysing and comparing the independent contributions of individual tropical SSTA modes on WNP TC frequency. The remainder of this paper is arranged as follows. Section 2 describes the data and methodology. Section 3 discusses the temporal relationship between basinwide WNP TC frequency and different SSTA indices. Sections 4 and 5 highlight the spatial changes in WNP TC genesis and environmental variables, respectively, as modulated by different SSTA modes. Section 6 examines anomalies of WNP TC genesis and environmental variables in 2005—a warm TNA year with ENM and IO SSTAs that were near average. Section 7 summarizes and concludes.

2 | DATA AND METHODOLOGY

WNP TC best track data are obtained from the International Best Track Archive for Climate Stewardship (IBTrACS) v4 dataset (Knapp et al., 2010). There are four warning agencies operationally providing TC best tracks over the full WNP, including the Joint Typhoon Warning Center (JTWC), the Japan Meteorological Agency (JMA), the China Meteorological Administration (CMA) and the Hong Kong Observatory (HKO). As suggested by Song and Klotzbach (2018), this study only considers TCs simultaneously recorded by all four agencies to minimize the uncertainty among data sources. Accordingly, this study identifies TC genesis as the first record that is simultaneously reported by all four agencies. TC genesis frequency (TCGF) is first obtained by counting TC genesis numbers over a $5^\circ \times 5^\circ$ grid and is then spatially smoothed through the method proposed by Kim et al. (2011).

This study focuses on the period from 1982 to 2022, because of the low reliability of TC observations due to lack of global satellite coverage prior to the early 1980s (Kossin et al., 2014). Another reason is that there is an interdecadal change in the relationship between WNP TC frequency and the ENM/IO/TNA indices (Cao et al., 2016; Liu & Chen, 2018; Zhan et al., 2014). All of these relationships were much weaker before the 1980s than they have been in more recent decades. Additionally, this study only considers the season spanning June–August (JJA), since the WNP TC frequency–ENM correlation is significant during the boreal summer but insignificant during the boreal autumn (Chen & Tam, 2010).

Monthly mean SST data over a $1^\circ \times 1^\circ$ grid are provided by the Hadley Centre Sea Ice and Sea Surface Temperature dataset (HadISST; Rayner et al., 2003). SSTAs are obtained by subtracting the corresponding long-term trends in SSTs from 1982 to 2022, to remove any global warming signal. Following Ashok et al. (2007), the ENM index is defined as

$$\text{ENM index} = \overline{\text{SSTA}}_C - 0.5 \times \overline{\text{SSTA}}_E - 0.5 \times \overline{\text{SSTA}}_W, \quad (1)$$

where the overbar denotes the area-averaged SSTA, which is computed over the three regions specified as the central (C: 165°E – 140°W , 10°S – 10°N), eastern (E: 110° – 70°W , 15°S – 5°N) and western (W: 125° – 145°W , 10°S – 20°N) tropical Pacific. The canonical ENSO, NIO and TNA indices are defined as SSTAs averaged over the Niño3.4 (170° – 120°W , 5°S – 5°N), NIO (50° – 100°E , 0° – 20°N) and TNA (80° – 25°W , 0° – 20°N) regions, respectively.

Monthly mean atmospheric conditions are obtained from the fifth generation European Centre for Medium-Range Weather Forecasts (ECMWF) reanalysis

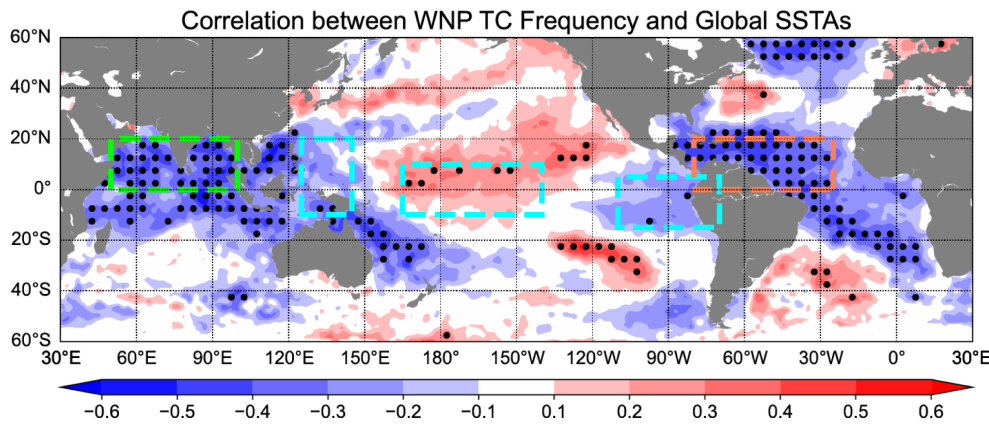


FIGURE 1 Correlation coefficient between basinwide WNP TC frequency and SSTAs during JJA from 1982 to 2022. The cyan, green and red rectangular boxes indicate the ENM, NIO and TNA regions that have significant correlations. Black dots denote correlations significant at the 0.05 level. [Colour figure can be viewed at wileyonlinelibrary.com]

of the global climate (ERA5; Hersbach et al., 2020), with a horizontal resolution of $0.25^\circ \times 0.25^\circ$. The genesis potential index (GPI) proposed by Emanuel and Nolan (2004) is estimated from the HadISST and ERA5 datasets. The GPI consists of four environmental variables: maximum potential intensity (MPI; Emanuel, 1988), 700–500-hPa relative humidity, 850-hPa absolute vorticity and 850–200-hPa VWS.

Statistical significance of correlation coefficients and regression coefficients is estimated based on a two-tailed Student's t test, while the effective sample size proposed by Bretherton et al. (1999) is used to account for autocorrelation of individual timeseries. To consider the sole impact of individual SSTA modes, this study applies the following equation:

$$x = c + b_{\text{CEN}}\tilde{I}_{\text{CEN}} + b_{\text{ENM}}\tilde{I}_{\text{ENM}} + b_{\text{NIO}}\tilde{I}_{\text{NIO}} + b_{\text{TNA}}\tilde{I}_{\text{TNA}} + \varepsilon. \quad (2)$$

Here, x represents any variable, c is a constant and ε is the residual. \tilde{I} denotes the normalized SSTA index, and b denotes its corresponding partial regression coefficients. The coefficients c and b are derived using multiple linear regression, while their significances are estimated by an F test.

Given the two possible pathways for linking TNA SSTAs to environmental changes over the WNP (Gao et al., 2018a, 2018b; Wang, 2019), responses in WNP TC activity to only one pathway are estimated by the following equations:

$$y = c + b_{\text{TNA-ENM}}\tilde{I}_{\text{TNA}} + b_{\text{NIO}}\tilde{I}_{\text{NIO}} + b_{\text{CEN}}\tilde{I}_{\text{CEN}} + \varepsilon, \quad (3)$$

$$y = c + b_{\text{TNA-NIO}}\tilde{I}_{\text{TNA}} + b_{\text{ENM}}\tilde{I}_{\text{ENM}} + b_{\text{CEN}}\tilde{I}_{\text{CEN}} + \varepsilon. \quad (4)$$

Here, y represents any TC metric, while other symbols are the same as in Equation (2). Note that $b_{\text{TNA-ENM}}$ and $b_{\text{TNA-NIO}}$ denote the influences of TNA SSTAs

through modulation of SSTAs over the NIO and the equatorial central Pacific, respectively.

3 | TEMPORAL CHANGE IN BASINWIDE WNP TC FREQUENCY

Figure 1 displays correlations between basinwide WNP TC frequency during JJA and simultaneous near-global SSTAs from 1982 to 2022. Consistent with Gao et al. (2020a, 2020b) and Yu et al. (2016b), significant negative correlations are concentrated over the NIO and TNA regions. Over the Pacific, an SST pattern resembling El Niño Modoki pattern is observed, with positive correlations over the central Pacific and negative correlations over the western and eastern Pacific. We also do not find a PMM-like SST pattern, which may be due to the insignificant relationship between WNP TC frequency and the PMM index in June and July (Fu et al., 2023). Figure 2 further highlights the notable interannual relationship between basinwide WNP TC frequency and the ENM ($r = 0.49$, $p < 0.01$), NIO ($r = -0.44$, $p < 0.01$) and TNA ($r = -0.43$, $p < 0.01$) indices. Consistent with earlier research, WNP TC frequency is greater during El Niño Modoki, cold NIO and cold TNA years than during La Niña Modoki, warm NIO and warm TNA years.

However, the changes in these three indices are not fully independent. Although the ENM and NIO indices only weakly correlate ($r = -0.24$, $p = 0.14$), they both significantly relate to the TNA index, with correlation coefficients of -0.48 ($p < 0.01$) and 0.47 ($p < 0.01$), respectively. Figure 3a shows that during an El Niño Modoki, significantly decreased SSTAs occur over the TNA, while SSTA changes are weak over the NIO. By comparison, a warm NIO is associated with not only a warm TNA but also a canonical El Niño (Figure 3c). There is a moderate correlation between the NIO and CEN indices ($r = 0.29$, $p = 0.07$). Consistent with Yang et al. (2022), both a La Niña Modoki structure and a

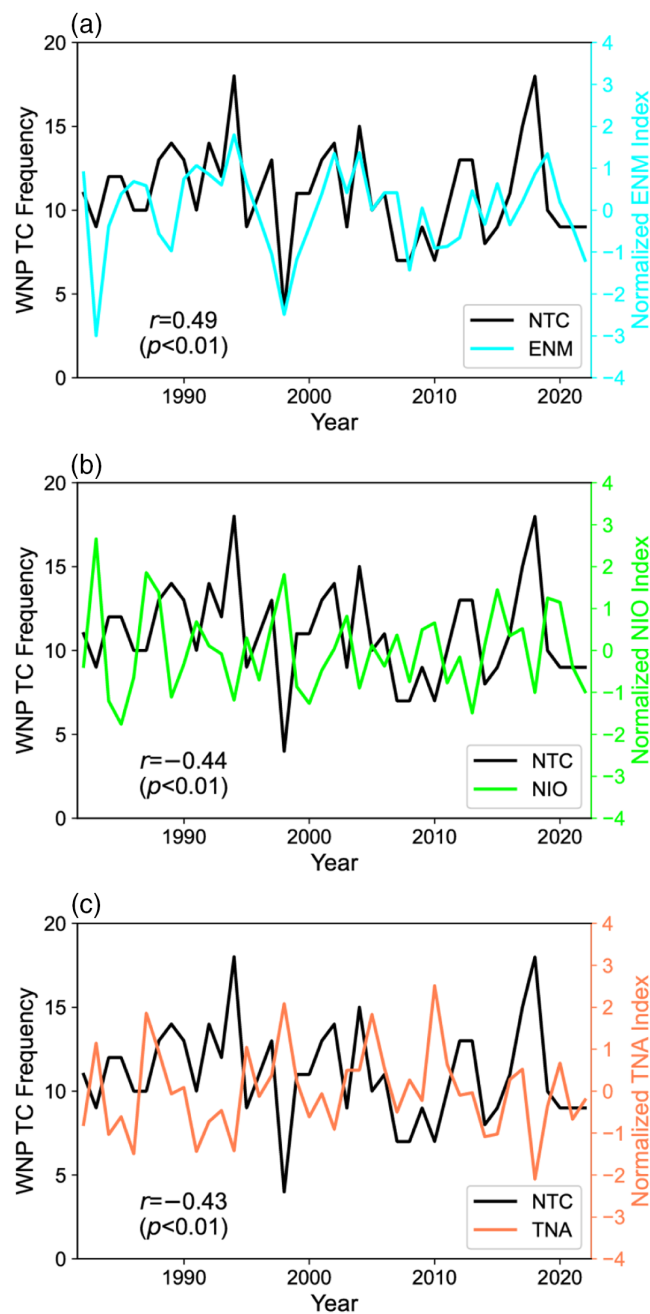


FIGURE 2 Annual changes in normalized (a) ENM, (b) NIO and (c) TNA indices during JJA between 1982 and 2022, as well as basinwide WNP TC frequency. Correlation coefficients and corresponding significance levels are given in each panel. [Colour figure can be viewed at [wileyonlinelibrary.com](https://onlinelibrary.wiley.com/doi/10.1002/joc.8417)]

warm NIO are observed during a warm TNA (Figure 3e). These results confirm the cross-basin interactions among the three basins, as reported in Wang (2019).

To obtain the independent impacts of SSTAs over individual basins, we next estimate partial regressions using Equation (2). Partial regressions generally maintain the typical SSTA pattern over the basin where the index predominates, but minimize the SSTA response in other

basins (Figure 3b,d,f). The only difference is that the regressions of SSTAs onto the ENM index are significantly negative over the western Pacific, while the partial regressions do not show these anomalies (Figure 3a,b). This result is likely caused by SST changes over the western Pacific being more related to SSTAs over the NIO than to the central-to-eastern Pacific, as shown in Figure 3c,d. The ENM index-related SSTA changes over the eastern Pacific are of a much greater magnitude than those over the western Pacific, regardless of whether we use the full regression or the partial regression. In addition, we also use Equations (3) and (4) to maintain one pathway for TNA SSTAs modulating SSTAs over other basins. As displayed in Figure 3g (Figure 3h), significant TNA SSTAs are associated with significant SSTA changes over the central Pacific (NIO).

We also perform partial regression on basinwide WNP TC frequency to measure the independent influence of these indices. Figure 4 displays what happens when all four indices are used as predictors. The resulting regression equation explains 37% of the total variance of basinwide TC frequency change. However, the regression coefficients of both the CEN and TNA indices are not significant. The insignificant CEN coefficient is a result of the weak correlation between basinwide WNP TC frequency and the CEN index ($r = 0.15$, $p = 0.34$). By contrast, the insignificant TNA coefficient conflicts with the significant basinwide WNP TC frequency–TNA correlation. Furthermore, when only the ENM and NIO indices are used as predictors, the explained variance of the regression equation (35%) only decreases slightly (Figure 4). These results imply that the contribution of TNA SSTAs to basinwide WNP TC frequency is already mostly included by using the ENM and NIO SSTAs. Consequently, the TNA index is likely not an independent variable for explaining WNP TC activity, given its close connection to the ENM and NIO indices.

Furthermore, the partial correlations of WNP TC frequency versus the ENM, NIO and TNA indices become 0.43 ($p < 0.01$), -0.38 ($p = 0.02$) and -0.04 ($p = 0.78$), respectively, if the effects of the other two indices are linearly removed. These results mean that the ENM (NIO) index independently explains 18% (14%) of the total variance in annual WNP TC frequency changes, with the TNA index by itself having almost no contribution. In addition, the partial correlation between WNP TC frequency and the TNA index is -0.22 ($p = 0.17$) [-0.24 ($p = 0.13$)] when removing the influence of the ENM (NIO) index. This implies that the two pathways of TNA SSTAs influencing environmental changes over the WNP are of comparable importance. The linkage of TNA SSTAs with WNP TC activity becomes insignificant if either of the pathways are excluded.

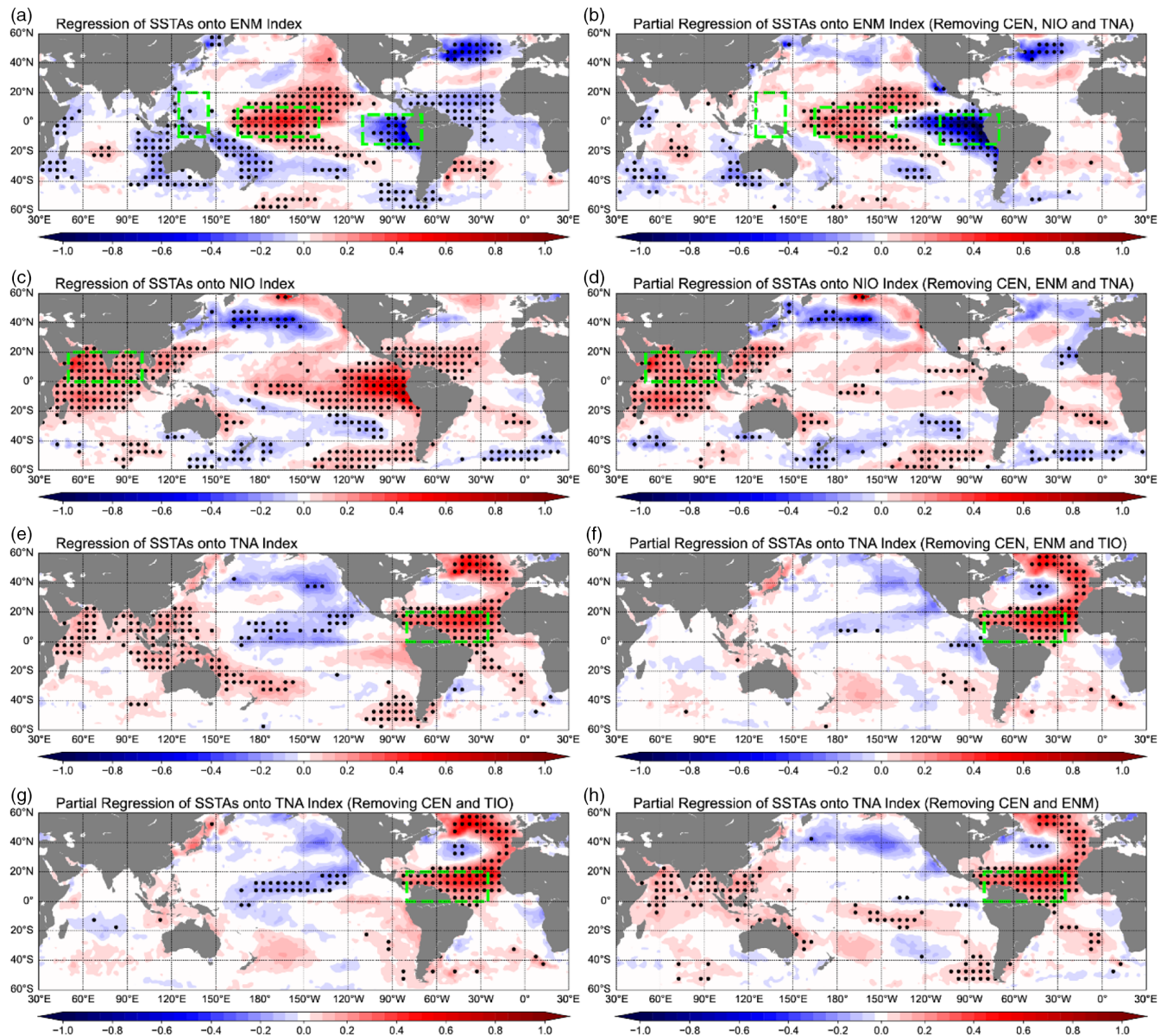


FIGURE 3 (a, c, e) Regressions and (b, d, f–h) partial regressions of near-global SSTAs (unit: $^{\circ}\text{C}$) onto the normalized (a, b) ENM, (c, d) NIO and (e–h) TNA indices from 1982 to 2022. Green boxes refer to the corresponding regions for identifying indices. Black dots denote the regressions or partial regressions significant at the 0.05 level. [Colour figure can be viewed at [wileyonlinelibrary.com](https://onlinelibrary.wiley.com)]

4 | SPATIAL CHANGE IN WNP TC GENESIS FREQUENCY

Figure 5a,c,e displays regressions of WNP TCGFs onto the ENM, NIO and TNA indices between 1982 and 2022. During an El Niño Modoki, TC genesis is enhanced over most of the WNP, with significantly increased TCGFs occurring east of 150°E (Figure 5a). During a warm NIO, TC genesis is suppressed over the subtropical WNP, with significantly decreased TCGFs north of 15°N and west of 155°E (Figure 5c). This significant region is shifted northwestward from the region with significant ENM-induced TCGF changes. During a warm TNA, there is suppressed

TC genesis over a northwest–southeast-oriented region of the WNP (Figure 5e). This TCGF distribution looks like a combination of TCGF changes in La Niña Modoki and in a warm NIO.

By comparison, Figure 5b,d,f displays partial regressions of WNP TCGFs onto the ENM, NIO and TNA indices, when the effects of the other indices are not considered. The pattern of ENM-induced TCGF anomalies remains almost unchanged, except that the magnitude of positive (negative) TCGFs decreases (increases) during an El Niño Modoki (Figure 5b). We next highlight two regions: Region A (145° – 175°E , 5° – 20°N) and Region B (125° – 145°E , 15° – 30°N). During an El Niño

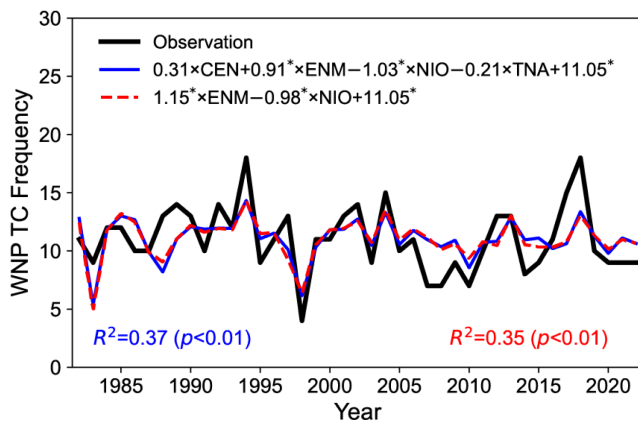


FIGURE 4 Observed and predicted WNP TC frequency during JJA between 1982 and 2022. The prediction equations are provided in the panel, which are obtained by using multiple linear regression. Their explained variances and the corresponding significance levels are also shown. Coefficients significant at the 0.05 level are noted with an asterisk in the prediction equations. [Colour figure can be viewed at [wileyonlinelibrary.com](https://onlinelibrary.wiley.com)]

Modoki, TC genesis is significantly enhanced over Region A but is slightly suppressed over Region B. Similarly, partial regressions of TCGFs onto the NIO index exhibit a similar distribution to the regressions of TCGFs, with a decreased (increased) magnitude of negative (positive) values (Figure 5d). During a warm NIO, Region A has slightly enhanced TC genesis, while Region B has significantly suppressed TC genesis. Note that although ENM and NIO SSTAs both significantly modulate basinwide TC frequency over the WNP, the regions in which their influences are the most significant are well separated.

By contrast, there are almost no significant warm TNA-induced TCGF changes over the WNP, after removing the influences of the CEN, ENM and NIO indices (Figure 5f). Weak TCGF decreases are observed over both Regions A and B. This implies that TNA SSTAs alone, unaccompanied by significant SSTAs over other tropical basins, only slightly modulates WNP TC genesis. Moreover, when retaining the influence of the ENM (NIO) index, partial regressions of TCGFs onto the TNA index exhibit a similar pattern to those onto the ENM (NIO) index (Figure 5g,h), with a pattern correlation coefficient of -0.43 ($p < 0.01$) [0.49 ($p < 0.01$)]. When the pathway linking TNA SSTAs to central Pacific (NIO) SSTAs is considered, WNP TC formation is significantly suppressed only over Region A (Region B) during a warm TNA, while it weakly changes over other subregions. This again implies that TNA SSTAs lead to basinwide changes in WNP TC formation through modulation of both NIO and Pacific SSTAs.

5 | CHANGES IN LARGE-SCALE ENVIRONMENTAL CONDITIONS

Figures 6–10 display partial regressions of environmental variables over the WNP onto the ENM, NIO and TNA indices. Full regression and correlation analysis has been shown in several previous studies (e.g., Gao et al., 2018a, 2018b; Liu & Chen, 2018; Zheng et al., 2016). Here, changes in 850-hPa relative vorticity are shown instead of 850-hPa absolute vorticity, since the Coriolis parameter is invariant with time. Figure 6 displays partial regressions of the GPI onto the three indices. These partial regressions are broadly consistent with those for TCGFs as shown in Figure 5b,d,f–h. During an El Niño Modoki, there are significant GPI increases over Region A and weak GPI changes over Region B (Figure 6a). During a warm NIO, significant GPI decreases are concentrated over Region B, while insignificant GPI changes occur over most of Region A (Figure 6b).

By contrast, the partial regressions of GPI onto the TNA index are of a smaller magnitude than those of the ENM and NIO indices (Figure 6c). These significant GPI changes occur near the equator and near the date-line, with almost no significant GPI changes over both Regions A and B. Gao et al. (2018a, 2018b) displayed regressions of the GPI directly onto the TNA index. During a warm TNA, GPI increases occur over a belt extending from the northern part of the South China Sea to the southeastern quadrant of the WNP, with GPI decreases occurring to the north and south. This pattern resembles the mirror image of the partial regressions of the GPI onto the ENM index (as shown in Figure 6a), likely resulting from a warm TNA-induced ENM-like SSTA pattern reported in Gao et al. (2018a, 2018b). Figure 6d,e presents the partial regressions of GPI onto the TNA index when retaining either of the influences of the ENM and NIO indices, which exhibits a similar pattern to the corresponding partial regressions of TCGF. When the influence of the ENM (NIO) index is retained, significantly decreased GPIs are observed over Region A (Region B) during a warm TNA, corresponding to suppressed TC formation. Note that the GPI pattern in Figure 6d (Figure 6e) is consistent with that in Figure 6a (Figure 6b), with a pattern correlation coefficient of -0.64 ($p < 0.01$) [0.89 ($p < 0.01$)]. This implies that environmental changes caused by TNA SSTAs through modulation of central Pacific (NIO) SSTAs are similar to those independently influenced by the ENM (NIO) index. Therefore, we focus on changes in environmental variables independently induced by the ENM, NIO and TNA indices in the following analysis.

The above findings imply that changes in TCGF induced by the three SSTA modes can be well captured by

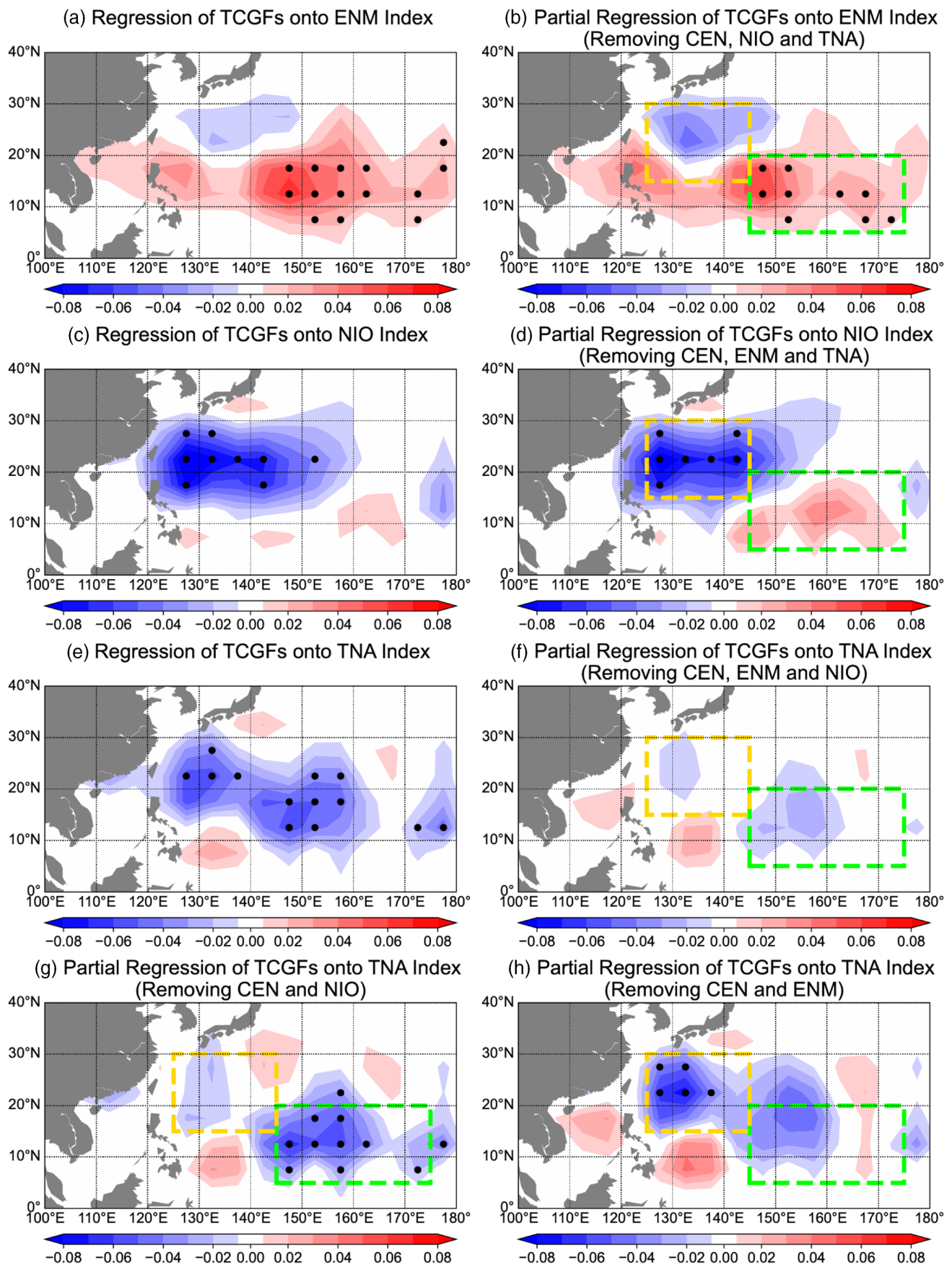


FIGURE 5 Legend on next page.

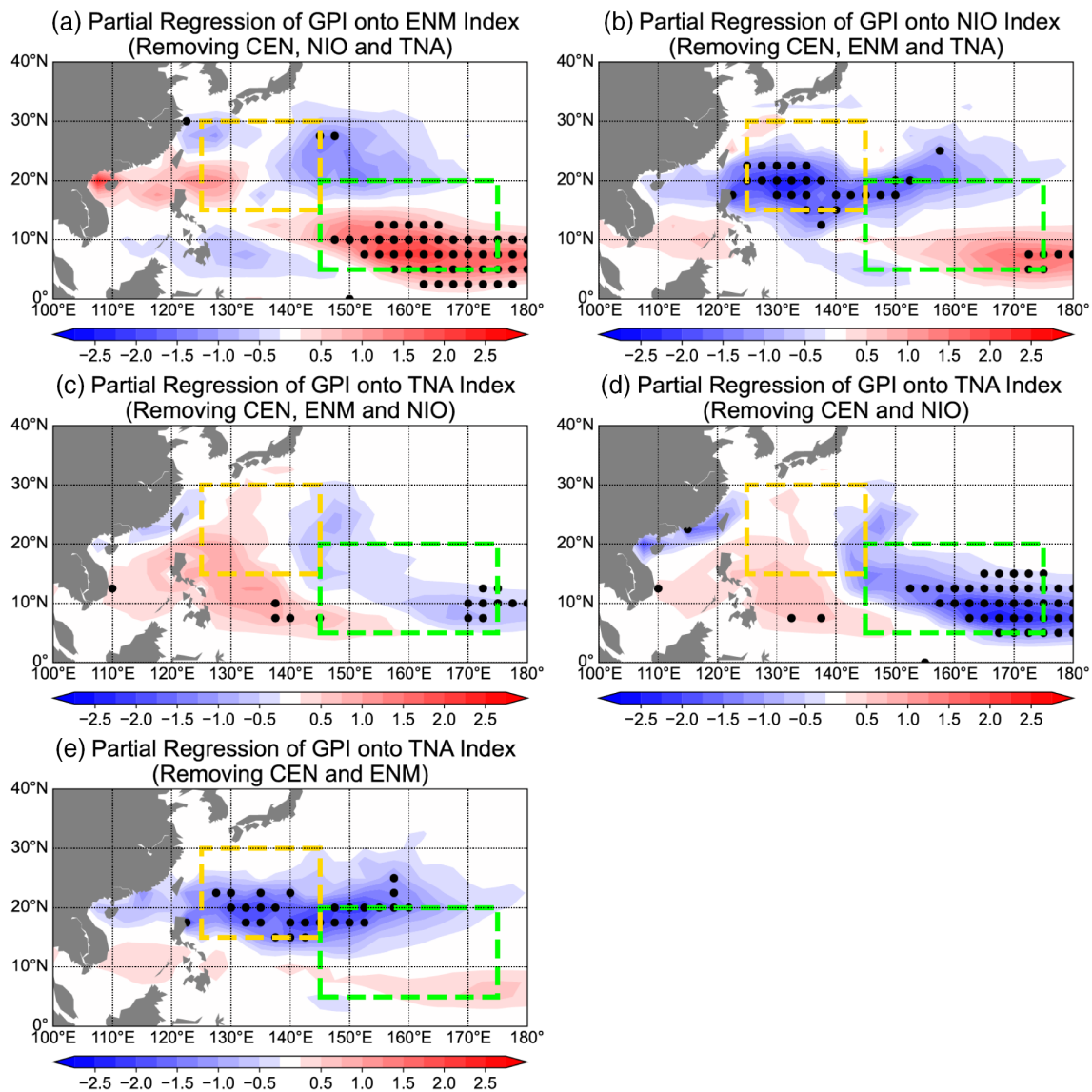


FIGURE 6 Partial regressions of GPI over the WNP onto the normalized (a) ENM, (b) NIO and (c–e) TNA indices from 1982 to 2022. Black dots denote partial regressions significant at the 0.05 level. Green and yellow dashed boxes denote the regions spanning 145°–175°E, 5°–20°N and 125°–145°E, 15°–30°N, respectively. [Colour figure can be viewed at [wileyonlinelibrary.com](https://onlinelibrary.com)]

the corresponding large-scale environment. Figures 7–9 display the partial regressions of four environmental variables constituting the GPI, including MPI, 700–500-hPa relative humidity, 850-hPa relative vorticity and 850–200-hPa VWS. During an El Niño Modoki, there are significant increases in MPI, relative humidity and relative vorticity with significant decreases in VWS over Region A, all favouring TC genesis (Figure 7). By comparison, weak changes in environmental factors occur over Region B.

During a warm NIO, there are almost no significant changes in environmental variables over Region A (Figure 8). Over Region B, there are only weak increases in MPI and VWS, with significant decreases in humidity occurring over the southern periphery (Figure 8a,b,d). Furthermore, there is a northeast–southwest-oriented region with significant vorticity decreases within 10°–20°N over the WNP, nearly covering all of Region B (Figure 8c). NIO SSTAs likely influence WNP TC genesis

FIGURE 5 (a, c, e) Regressions and (b, d, f–h) partial regressions of WNP TCGFs onto the normalized (a, b) ENM, (c, d) NIO and (e–h) TNA indices from 1982 to 2022. Black dots denote regressions or partial regressions significant at the 0.05 level. Green and yellow dashed boxes denote the regions spanning 145°–175°E, 5°–20°N and 125°–145°E, 15°–30°N, respectively. [Colour figure can be viewed at [wileyonlinelibrary.com](https://onlinelibrary.com)]

Partial Regression of Environmental Variables onto ENM Index

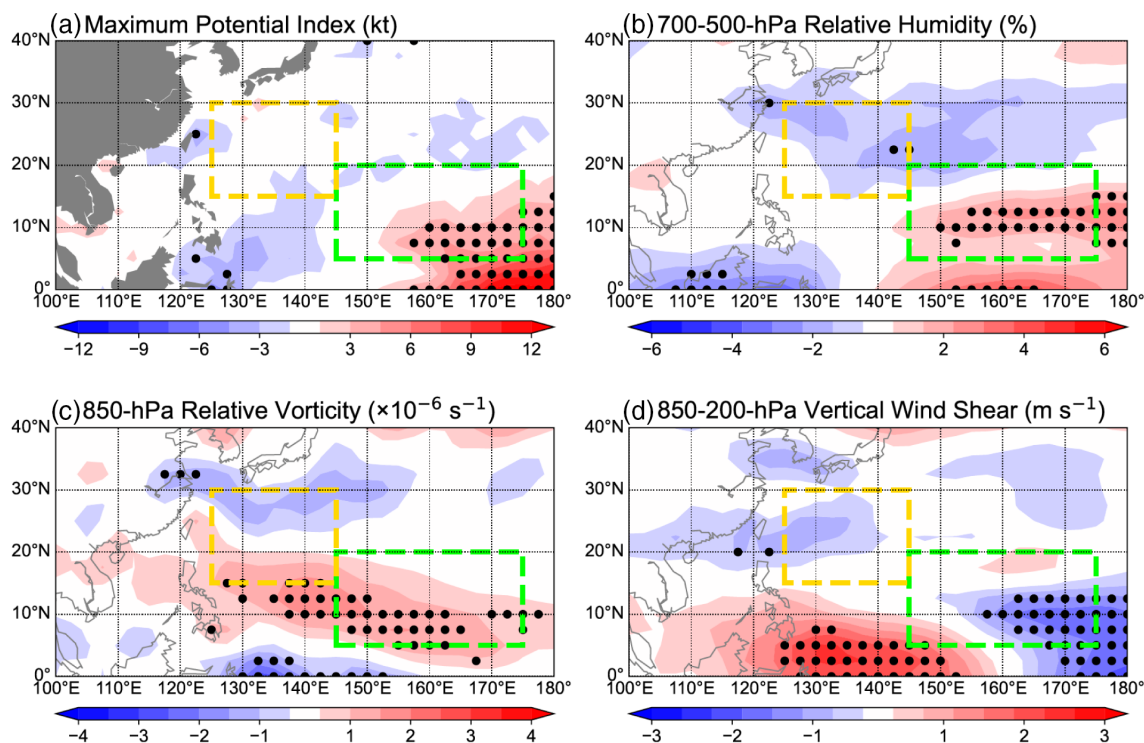


FIGURE 7 Partial regressions of (a) MPI, (b) 700–500-hPa relative humidity, (c) 850-hPa relative vorticity and (d) 850–200-hPa VWS onto the normalized ENM index from 1982 to 2022. Black dots denote partial regressions significant at the 0.05 level. Green and yellow dashed boxes denote regions spanning 145°–175°E, 5°–20°N and 125°–145°E, 15°–30°N, respectively. [Colour figure can be viewed at [wileyonlinelibrary.com](https://onlinelibrary.wiley.com)]

primarily through modulations of low-level relative vorticity over the WNP, as noted in previous publications (e.g., Tao et al., 2012; Zhan et al., 2011a). Consistent with weak changes in GPI, during a warm TNA, there are almost no significant changes in all four environmental factors over both Regions A and B (Figure 9). In particular, relative vorticity is only slightly reduced over both regions (Figure 9c). This further implies that the TNA SSTA by itself only slightly modulates the large-scale WNP environment.

Given that changes in TCGF and GPI over both Regions A and B correspond well to changes in low-level relative vorticity, Figure 10 further displays partial regressions of the 850-hPa flow. During an El Niño Modoki, maximum SSTA increases occur over the equatorial central Pacific, triggering anomalously deep convection there. This anomalously deep convection can generate a westward-propagating Rossby wave, which induces significant anomalous low-level westerlies over the equatorial WNP (Figure 10a). Subsequently, there is an anomalous large-scale cyclonic circulation north of 20°N over the WNP, with its centre located in Region A. This anomalous large-scale cyclonic circulation provides positive relative vorticity, favouring TC development. By comparison, during a warm NIO, the peak SSTA

increases that occur over the NIO can generate anomalous convection associated with a local anomalous low-level cyclone (Figure 10b). Significant anomalous low-level easterlies induced by an eastward-propagating Kelvin wave extend from the NIO to the WNP and are concentrated between the equator and 10°N. As a result, an anomalous large-scale anticyclonic circulation occurs over the subtropical WNP, centred over Region B. This leads to negative vorticity anomalies, which suppresses TC genesis. When comparing the locations of the anomalous flow over the WNP, the anomalous anticyclone (cyclone) is shifted westward (eastward) during a warm NIO (an El Niño Modoki) (Figure 10a,b), due to the shifts in where the maximum SSTA increases occur. The warm NIO-induced anomalous anticyclone is more poleward than the El Niño Modoki-induced anomalous cyclone. As a result, the anomalous easterlies shift more northward than the anomalous westerlies.

When excluding the impacts of the ENM and NIO SSTAs, significant changes in the 850-hPa flow during a warm TNA only occur over an off-equatorial region extending from the central Pacific to the western Atlantic (Figure 10c). Anomalous low-level westerlies are found

Partial Regression of Environmental Variables onto NIO Index

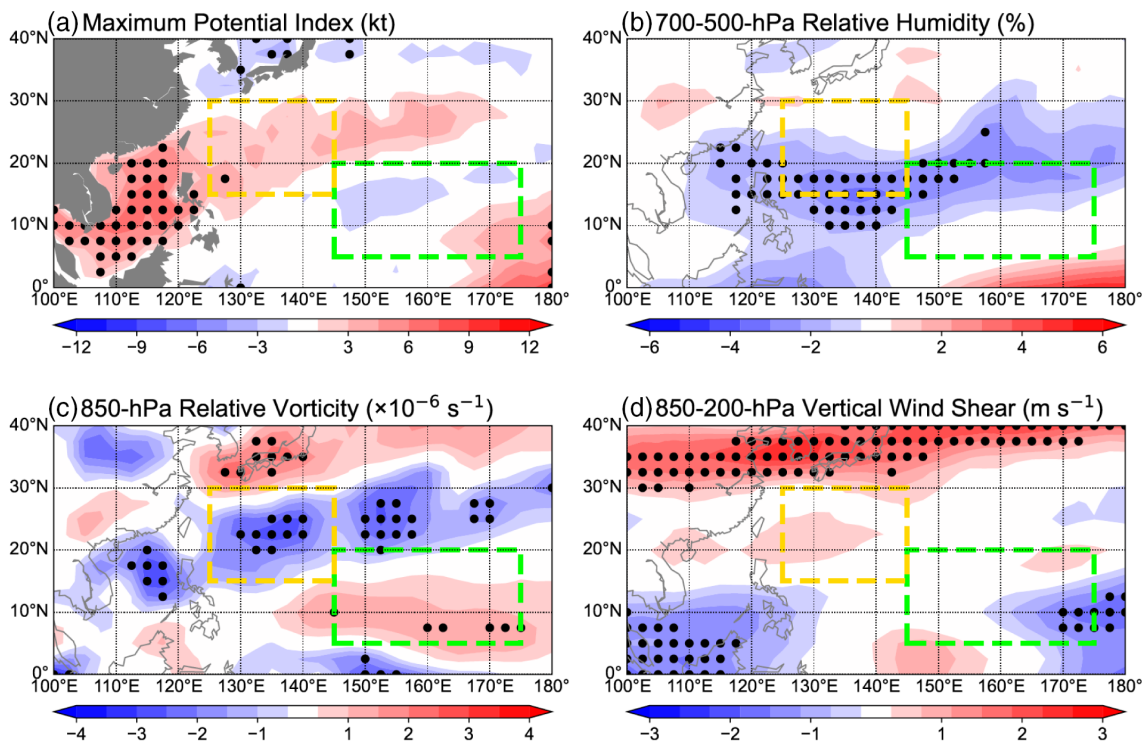


FIGURE 8 As in Figure 7, but for partial regressions onto the normalized NIO index. [Colour figure can be viewed at wileyonlinelibrary.com]

Partial Regression of Environmental Variables onto TNA Index

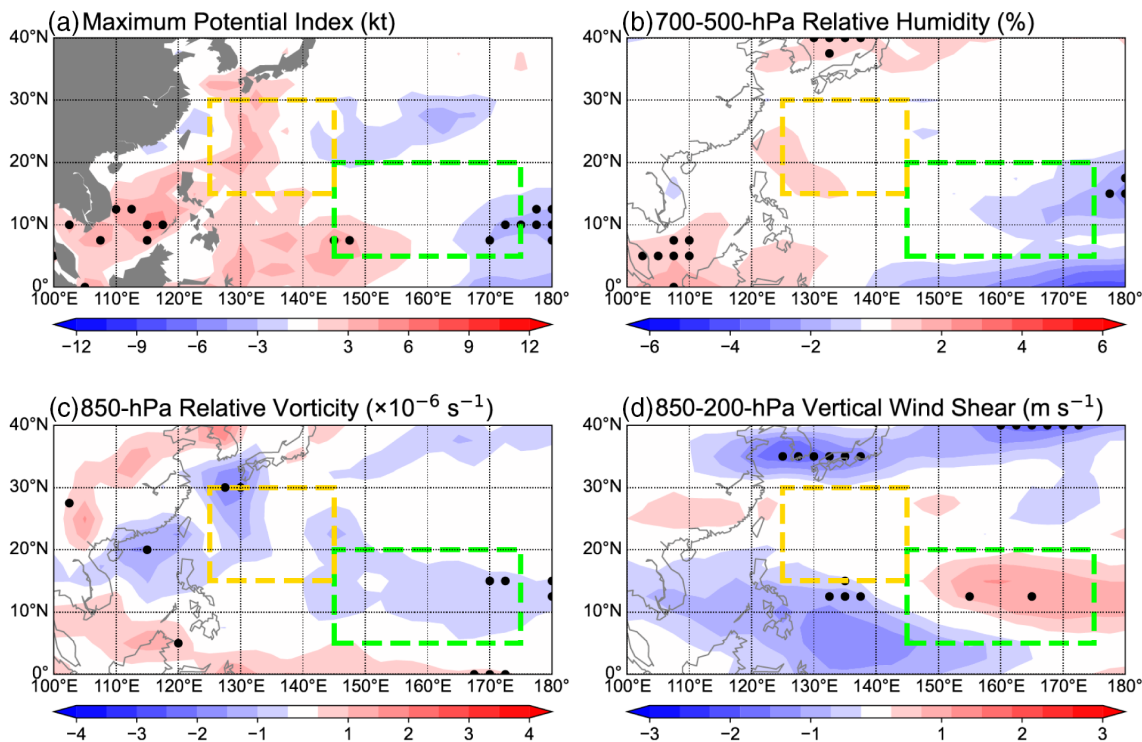


FIGURE 9 As in Figure 7, but for partial regressions onto the normalized TNA index. [Colour figure can be viewed at wileyonlinelibrary.com]

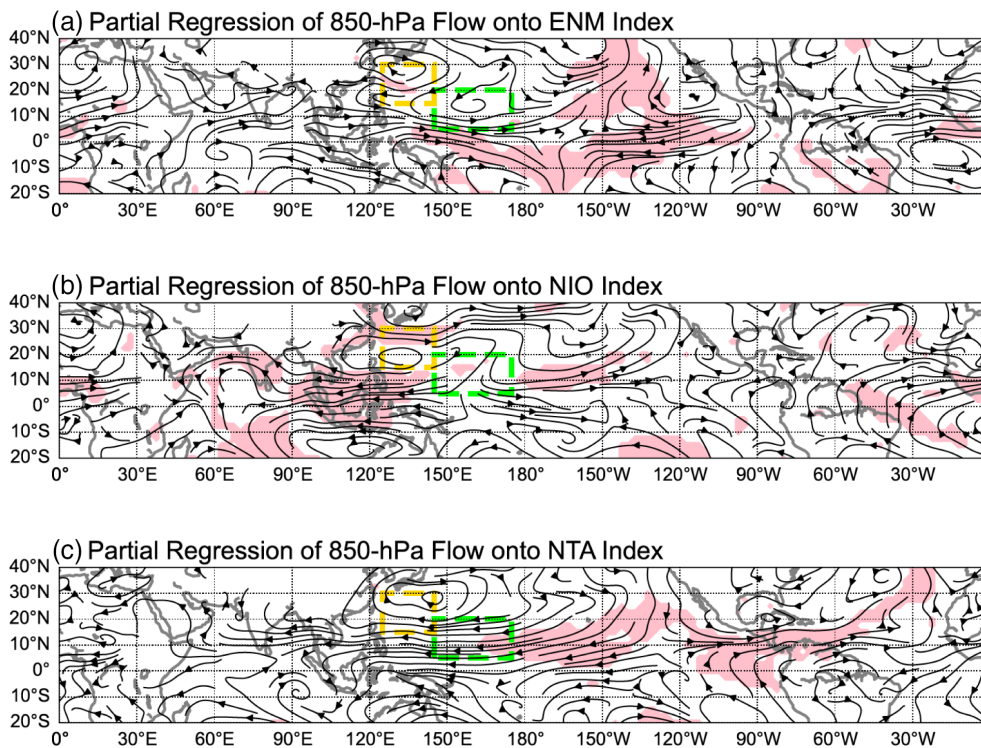


FIGURE 10 Partial regressions of 850-hPa horizontal flow on the normalized (a) ENM, (b) NIO and (c) TNA indices between 1982 and 2022. Pink areas denote partial regressions significant at the 0.05 level. Green and yellow dashed boxes denote the regions spanning 145°–175°E, 5°–20°N and 125°–145°E, 15°–30°N, respectively. [Colour figure can be viewed at [wileyonlinelibrary.com](https://onlinelibrary.wiley.com/doi/10.1002/joc.8417)]

between the eastern Pacific and the western Atlantic, indicating an anomalous Walker circulation triggered by the peak SSTA increases over the TNA. There is divergent flow spanning 150°–120°W, corresponding to a descending branch of the anomalous Walker cell. This further results in anomalous easterlies over the off-equatorial central-to-western Pacific. The significance of these anomalous easterlies decreases westward, owing to the increasing distance to the centre of the divergent flow. Although an anomalous low-level anticyclone occurs over the WNP, the flow anomalies that it generates are mostly insignificant. This leads to only weak changes in WNP relative vorticity.

6 | DISCUSSION

The above results are based on partial regression analysis, which considers the independent contributions of one factor by statistically removing the contributions of others. To confirm these findings, we now evaluate changes in WNP TC genesis and environmental conditions during JJA of 2005. 2005 was an extremely warm TNA phase, with a TNA index exceeding 1.8 standard deviations. At the same time, the ENM and NIO indices were less than 0.2 standard deviations. Figure 11a highlights that during JJA of 2005, most of the significant SSTAs occurred over the Atlantic, while almost no significant SSTAs occurred over other basins. Ten TCs formed

in JJA over the WNP, slightly less than the climatological average of 11 TCs. Although WNP TCGF anomalies had a west–east dipolar distribution, these anomalies were all statistically insignificant (Figure 11b). In addition, the 850-hPa flow anomalies in 2005 showed a similar pattern to the partial regressions onto the TNA index, with significant flow anomalies mainly concentrated from the eastern Pacific to the western Atlantic (Figure 11c). Over the WNP, there was an insignificant anomalous low-level anticyclonic circulation, which likely only slightly modulated TC genesis due to its weak intensity.

7 | CONCLUSION

This study investigates the contributions of three tropical SSTA modes to interannual changes in summertime WNP TC frequency from 1982 to 2022. Given the close interactions among tropical basins, partial regressions of TC metrics and environmental variables onto the three SSTA indices are applied to consider the independent influences of the different modes. Basinwide WNP TC frequency significantly correlates with both the ENM and NIO indices, regardless of whether the influences of the other indices are considered. The ENM and NIO indices independently explain 18% and 14% of the total variance in the annual WNP TC frequency change, respectively. Moreover, although there are basinwide changes in WNP TC genesis induced by both the ENM and NIO SSTAs,

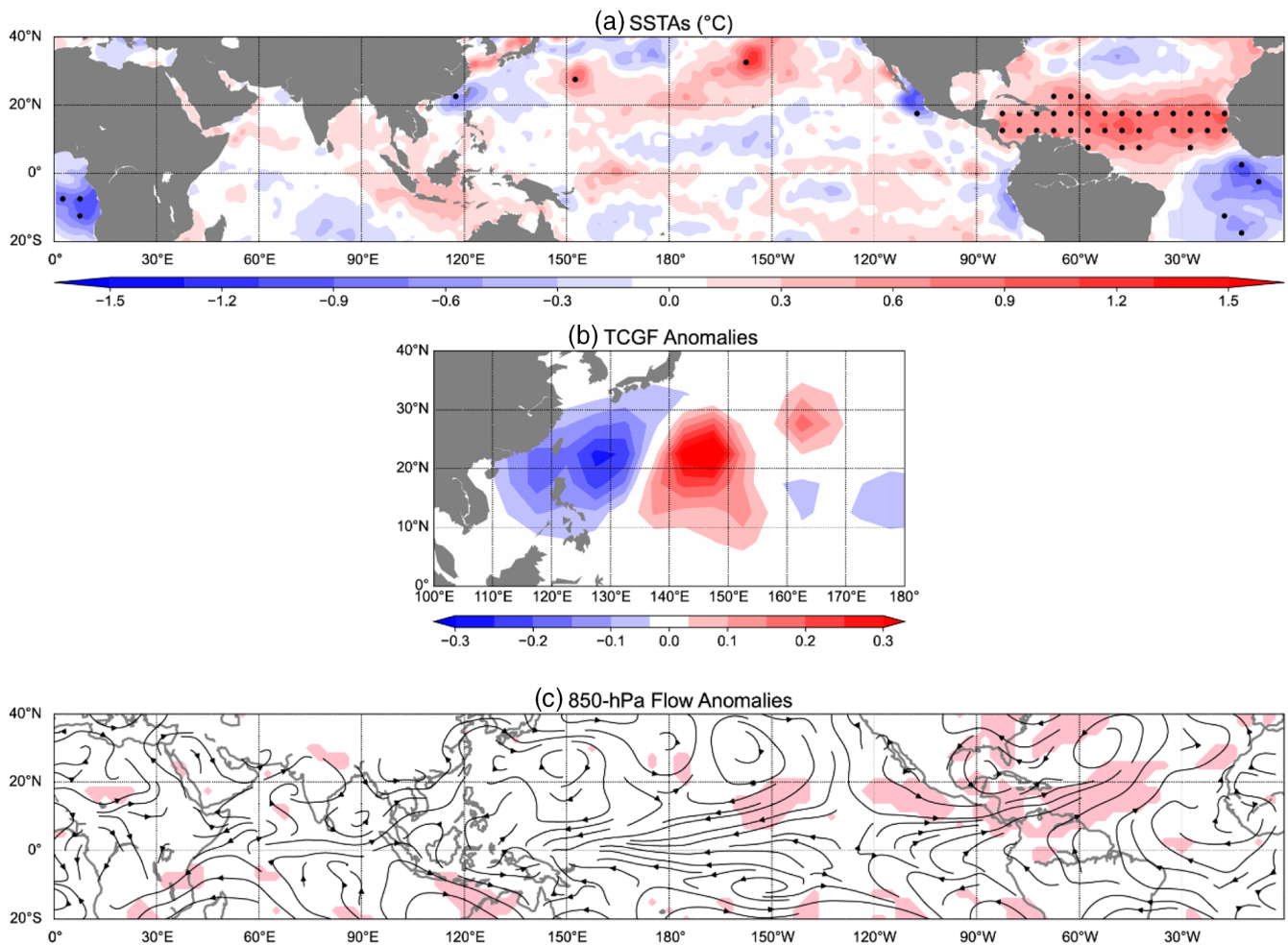


FIGURE 11 Anomalies of (a) SSTA, (b) TCGF and (c) 850-hPa flow in JJA 2005. Anomalies significant at the 0.05 level based on a Student's *t* test are marked with black dots in (a) and (b) with pink shading in (c). [Colour figure can be viewed at wileyonlinelibrary.com]

the regions with the most significant changes are well separated. During an El Niño Modoki (a warm NIO), significant TCGF increases (decreases) are observed over the southeastern (northwestern) part of the WNP.

By contrast, the significant TC frequency-TNA correlation is primarily a result of the significant relationship between the TNA index and the ENM and NIO indices. The modulation of TNA SSTAs on basinwide WNP TC frequency becomes insignificant when the impacts of other SSTA modes are excluded. Furthermore, the partial correlation between WNP TC frequency and the TNA index when only removing the ENM effect is of a similar value to that when only removing the NIO SSTA effect, which implies that the two pathways of TNA SSTAs influencing environmental changes over the WNP are of comparable importance. The linkage of TNA SSTAs on WNP TC activity becomes insignificant if either of the pathways is excluded. In addition, only weak changes in TCGF are observed over the WNP if the sole effect of TNA SSTAs is considered. When only retaining the

influence of the ENM (NIO) index, partial regressions of TCGFs onto the TNA index exhibit a similar pattern to those onto the ENM (NIO) index. When the pathway linking TNA SSTAs to central Pacific (NIO) SSTAs is considered, WNP TC formation is significantly suppressed over the southeastern (northwestern) part of the WNP during a warm TNA, while it changes weakly over other subregions.

The above changes in TCGF can be well captured by changes in the GPI. During an El Niño Modoki, significantly enhanced TC genesis over Region A (145°–175°E, 5°–20°N) is linked to a combined increase in MPI, 700–500-hPa relative humidity and 850-hPa relative vorticity as well as decreased VWS. Anomalous convection triggered by the warm equatorial central Pacific induces westward-propagating Rossby waves, which are associated with anomalous westerlies near the equator and an anomalous cyclone over the WNP, favouring TC genesis. By comparison, during a warm NIO, TC genesis is significantly suppressed over Region

B (125°–145°E, 15°–30°N), primarily because of significant decreases in relative vorticity. Warm NIO SSTAs can also trigger anomalous convection over the NIO, generating eastward-propagating Kelvin waves associated with anomalous easterlies in the off-equatorial belt from the NIO to the WNP. This further induces an anomalous anticyclone centred over the subtropical WNP, inhibiting TC development. However, during a warm TNA, no notable changes in environmental variables are found over most of the WNP. The significant flow anomalies that are solely induced by TNA SSTAs are limited to the central-to-eastern Pacific and the western Atlantic, with only weak flow changes occurring over the WNP. This implies that TNA SSTAs have only a minor impact on modulating the WNP environment if related SSTA changes occurring in other basins are not taken into consideration.

Our study highlights the distinct regions with significant TCGF changes induced by ENM and NIO SSTAs. These changes are primarily caused by the anomalous low-level anticyclone (cyclone) over the WNP shifting westward (eastward) during a warm NIO (an El Niño Modoki), due to shifts in where the maximum SSTA increases occur. Our study confirms that TNA SSTAs can modulate WNP TC genesis through two pathways influencing SSTAs over the Pacific and IO, respectively (e.g., Gao et al., 2018a, 2018b; Huo et al., 2015; Wang, 2019; Yu et al., 2016a). The signal related to TNA SSTAs has difficulty propagating into the WNP without the canonical response from other oceans. As opposed to earlier publications which looked at just one pathway for TNA SSTs influencing the WNP environment (e.g., Huo et al., 2015; Yu et al., 2016a), our study shows that the two pathways of TNA SSTAs influencing the WNP environment are of comparable importance. If either of the pathways is excluded, the significant modulation of TNA SSTAs on WNP TC formation is limited to a small subregion, while the correlation between the TNA index and basinwide WNP frequency is largely reduced and becomes insignificant. Note that the pathways of TNA SSTAs modulating central Pacific and NIO SSTAs are considered the primary mechanism of how TNA SSTAs influence WNP TC activity in Huo et al. (2015) and Yu et al. (2016a), respectively. Huo et al. (2015) focused on the lag relationship between TNA SSTAs in the preceding boreal spring (March–May) and WNP TC activity in June–October, while Yu et al. (2016a) examined the simultaneous relationship between TNA SSTAs and WNP TC activity during July–October. It is likely that the relative importance of the above two pathways of TNA SSTAs changes with the season being investigated. This needs to be investigated in a future work.

AUTHOR CONTRIBUTIONS

Jinjie Song: Conceptualization; methodology; investigation; supervision; writing – original draft; writing – review and editing. **Philip J. Klotzbach:** Formal analysis; writing – review and editing. **Nannan Qin:** Methodology; software. **Yihong Duan:** Funding acquisition; supervision.

ACKNOWLEDGEMENTS

This work was jointly funded by the National Natural Science Foundation of China (U2342203, 42192554, 61827901, 42175007, 41905001 and 42192552). Klotzbach would like to acknowledge financial support from the G. Unger Vetlesen Foundation.

DATA AVAILABILITY STATEMENT

All data used in this study are freely available online. Western North Pacific TC best track data provided in IBTrACS are available at: <https://www.ncei.noaa.gov/products/international-best-track-archive?name=ib-v4-access>. Monthly mean SST data provided by the Hadley Centre Sea Ice and Sea Surface Temperature (HadISST) are obtained from: <https://www.metoffice.gov.uk/hadobs/hadist/data/download.html>. The fifth generation European Centre for Medium–Range Weather Forecasts atmospheric reanalysis of the global climate (ERA5) is retrieved from: <https://cds.climate.copernicus.eu/cdsapp#!/dataset/reanalysis-era5-pressure-levels-monthly-means?tab=form>.

ORCID

Jinjie Song  <https://orcid.org/0000-0003-3948-8894>

Nannan Qin  <https://orcid.org/0000-0001-7036-879X>

REFERENCES

- Ashok, K., Behera, S. K., Rao, S. A., Weng, H., & Yamagata, T. (2007). El Niño Modoki and its possible teleconnection. *Journal of Geophysical Research*, 112, C11007.
- Bretherton, C.S., Widmann, M., Dymnikov, V.P., Wallace, J.M. & Blade, I. (1999) The effective number of spatial degrees of freedom of a time-varying field. *Journal of Climate*, 12, 1990–2009.
- Cao, X., Chen, S., Chen, G. & Wu, R. (2016) Intensified impact of northern tropical Atlantic SST on tropical cyclogenesis frequency over the western North Pacific after the late 1980s. *Advances in Atmospheric Sciences*, 33, 919–930.
- Capotondi, A., Wittenberg, A.T., Newman, M., Di Lorenzo, E., Yu, J., Braconnot, P. et al. (2015) Understanding ENSO diversity. *Bulletin of the American Meteorological Society*, 96, 921–938.
- Chan, J.C.L. (1985) Tropical cyclone activity in the northwest Pacific in relation to the El Niño/Southern Oscillation phenomenon. *Monthly Weather Review*, 113, 599–606.
- Chan, J.C.L. (2000) Tropical cyclone activity over the western North Pacific associated with El Niño and La Niña events. *Journal of Climate*, 13, 2960–2972.

- Chen, G. & Tam, C.-Y. (2010) Different impacts of two kinds of Pacific Ocean warming on tropical cyclone frequency over the western North Pacific. *Geophysical Research Letters*, 37, L01803.
- Du, Y., Yang, L. & Xie, S.P. (2011) Tropical Indian Ocean influence on Northwest Pacific tropical cyclones in summer following strong El Niño. *Journal of Climate*, 24, 315–322.
- Emanuel, K. (2018) 100 years of progress in tropical cyclone research. In: *A century of progress in atmospheric and related sciences: celebrating the American Meteorological Society centennial*, Vol. 59. American Meteorological Society, pp. 15.1–15.68. <https://doi.org/10.1175/AMSMONOGRAPHIS-D-18-0016.1>
- Emanuel, K.A. (1988) The maximum intensity of hurricanes. *Journal of Atmospheric Sciences*, 45, 1143–1155.
- Emanuel, K.A. & Nolan, D.S. (2004) Tropical cyclone activity and global climate. In: *26th conference on hurricanes and tropical meteorology*. Miami, FL: American Meteorological Society, pp. 240–241.
- Fu, M., Wang, C., Wu, L. & Zhao, H. (2023) Season-dependent modulation of Pacific meridional mode on tropical cyclone genesis over the western North Pacific. *Journal of Geophysical Research: Atmospheres*, 128, e2022JD037575.
- Gao, J., Zhao, H., Klotzbach, P.J., Wang, C., Raga, G.B. & Chen, S. (2020a) Possible influence of tropical Indian Ocean sea surface temperature on the proportion of rapidly intensifying western North Pacific tropical cyclones during the extended boreal summer. *Journal of Climate*, 33, 9129–9143.
- Gao, S., Chen, Z. & Zhang, W. (2018a) Impacts of tropical North Atlantic SST on western North Pacific landfalling tropical cyclones. *Journal of Climate*, 31, 853–862.
- Gao, S., Zhu, L., Zhang, W. & Chen, Z. (2018b) Strong modulation of the Pacific meridional mode on the occurrence of intense tropical cyclones over the western North Pacific. *Journal of Climate*, 31, 7739–7749.
- Gao, S., Zhu, L., Zhang, W. & Shen, X. (2020b) Impact of the Pacific meridional mode on landfalling tropical cyclone frequency in China. *Quarterly Journal of the Royal Meteorological Society*, 146, 2410–2420.
- Gill, A.E. (1980) Some simple solutions for heat-induced tropical circulation. *Quarterly Journal of the Royal Meteorological Society*, 106, 447–462.
- Ha, Y., Zhong, Z., Yang, X. & Sun, Y. (2015) Contribution of East Indian Ocean SSTA to western North Pacific tropical cyclone activity under El Niño/La Niña conditions. *International Journal of Climatology*, 35, 506–519.
- Hersbach, H., Bell, B., Berrisford, P., Hirahara, S., Horányi, A., Muñoz-Sabater, J. et al. (2020) The ERA5 global reanalysis. *Quarterly Journal of the Royal Meteorological Society*, 146, 1999–2049.
- Huo, L., Guo, P., Hameed, S.N. & Jin, D. (2015) The role of tropical Atlantic SST anomalies in modulating western North Pacific tropical cyclone genesis. *Geophysical Research Letters*, 42, 2378–2384.
- Jin, R., Yu, H., Wu, Z. & Zhang, P. (2022) Impact of the North Atlantic sea surface temperature tripole on the northwestern Pacific weak tropical cyclone frequency. *Journal of Climate*, 35, 3057–3074.
- Kao, H. & Yu, J. (2009) Contrasting Eastern–Pacific and Central–Pacific types of ENSO. *Journal of Climate*, 22, 615–632.
- Kim, H.-M., Webster, P.J. & Curry, J.A. (2011) Modulation of North Pacific tropical cyclone activity by three phases of ENSO. *Journal of Climate*, 24, 1839–1849.
- Knapp, K.R., Kruk, M.C., Levinson, D.H., Diamond, H.J. & Neumann, C.J. (2010) The international best track archive for climate stewardship (IBTrACS). *Bulletin of the American Meteorological Society*, 91, 363–376.
- Kossin, J.P., Emanuel, K.A. & Vecchi, G.A. (2014) The poleward migration of the location of tropical cyclone maximum intensity. *Nature*, 509, 349–352.
- Lander, M.A. (1994) An exploratory analysis of the relationship between tropical storm formation in the western North Pacific and ENSO. *Monthly Weather Review*, 122, 636–651.
- Lee, T.-C., Knutson, T.R., Kamahori, H. & Ying, M. (2012) Impacts of climate change on tropical cyclones in the western North Pacific basin. Part I: past observations. *Tropical Cyclone Research and Review*, 1, 213–230.
- Li, C. & Wang, C. (2014) Simulated impacts of two types of ENSO events on tropical cyclone activity in the western North Pacific: large-scale atmospheric response. *Climate Dynamics*, 42, 2727–2743.
- Li, R.C.Y. & Zhou, W. (2012) Changes in western Pacific tropical cyclones associated with the El Niño–Southern Oscillation cycle. *Journal of Climate*, 25, 5864–5878.
- Liu, Y. & Chen, G. (2018) Intensified influence of the ENSO Modoki on boreal summer tropical cyclone genesis over the western North Pacific since the early 1990s. *International Journal of Climatology*, 38, e1258–e1265.
- Patricola, C.M., Camargo, S.J., Klotzbach, P.J., Saravanan, R. & Chang, P. (2018) The influence of ENSO flavors on western North Pacific tropical cyclone activity. *Journal of Climate*, 31, 5395–5416.
- Rayner, N.A., Parker, D.E., Horton, E.B., Folland, C.K., Alexander, L.V., Rowell, D.P. et al. (2003) Global analyses of sea surface temperature, sea ice, and night marine air temperature since the late nineteenth century. *Journal of Geophysical Research: Atmospheres*, 108, 4407.
- Saunders, M.A., Chandler, R.E., Merchant, C.J. & Roberts, F.P. (2000) Atlantic hurricanes and NW Pacific typhoons: ENSO spatial impacts on occurrence and landfall. *Geophysical Research Letters*, 27, 1147–1150.
- Song, J. & Klotzbach, P.J. (2018) What has controlled the poleward migration of annual averaged location of tropical cyclone lifetime maximum intensity over the western North Pacific since 1961? *Geophysical Research Letters*, 45, 1148–1156.
- Tao, L., Wu, L., Wang, Y. & Yang, J. (2012) Influence of tropical Indian Ocean warming and ENSO on tropical cyclone activity over the western North Pacific. *Journal of the Meteorological Society of Japan*, Series II, 90, 127–144.
- Timmermann, A., An, S.I., Kug, J.S., Jin, F.F., Cai, W., Capotondi, A. et al. (2018) El Niño–Southern Oscillation complexity. *Nature*, 559, 535–545.
- Walsh, K.J.E., McBride, J.L., Klotzbach, P.J., Balachandran, S., Camargo, S.J., Holland, G. et al. (2016) Tropical cyclones and climate change. *Wiley Interdisciplinary Reviews: Climate Change*, 7, 65–89.
- Wang, B. & Chan, J.C.L. (2002) How strong ENSO events affect tropical storm activity over the western North Pacific. *Journal of Climate*, 15, 1643–1658.

- Wang, C. (2019) Three-ocean interactions and climate variability: a review and perspective. *Climate Dynamics*, 53, 5119–5136.
- Wang, C., Li, C., Mu, M. & Duan, W. (2013) Seasonal modulations of different impacts of two types of ENSO events on tropical cyclone activity in the western North Pacific. *Climate Dynamics*, 40, 2887–2902.
- Wang, C. & Wang, B. (2019) Tropical cyclone predictability shaped by western Pacific subtropical high: integration of trans-basin sea surface temperature effects. *Climate Dynamics*, 53, 2697–2714.
- Wu, Q., Zhao, J., Zhan, R. & Gao, J. (2020) Revisiting the interannual impact of the Pacific meridional mode on tropical cyclone genesis frequency in the Western North Pacific. *Climate Dynamics*, 56, 1003–1015.
- Xie, S.-P. (1999) A dynamic ocean-atmosphere model of the tropical Atlantic decadal variability. *Journal of Climate*, 12, 64–70.
- Xie, S.-P., Hu, K., Hafner, J., Tokinaga, H., Du, Y., Huang, G. et al. (2009) Indian Ocean capacitor effect on Indo-western Pacific climate during the summer following El Niño. *Journal of Climate*, 22, 730–747.
- Xie, S.-P., Kosaka, Y., Du, Y., Hu, K., Chowdary, J.S. & Huang, G. (2016) Indo-western Pacific ocean capacitor and coherent climate anomalies in post-ENSO summer: a review. *Advances in Atmospheric Sciences*, 33, 411–432.
- Xie, S.-P. & Philander, S.G.H. (1994) A coupled ocean-atmosphere model of relevance to the ITCZ in the eastern Pacific. *Tellus A*, 46, 340–350.
- Yang, Y.-M., Park, J.-H., An, S.-I., Yeh, S.-W., Zhu, Z., Liu, F. et al. (2022) Increased Indian Ocean-North Atlantic Ocean warming chain under greenhouse warming. *Nature Communications*, 13, 3978.
- Yu, J., Li, T., Tan, Z. & Zhu, Z. (2016a) Effects of tropical North Atlantic SST on tropical cyclone genesis in the western North Pacific. *Climate Dynamics*, 46, 865–877.
- Yu, J.H., Chen, C., Li, T., Zhao, X., Xue, H. & Sun, Q. (2016b) Contribution of major SSTA modes to the climate variability of tropical cyclone genesis frequency over the western North Pacific. *Quarterly Journal of the Royal Meteorological Society*, 142, 1171–1181.
- Zhan, R., Wang, Y. & Lei, X. (2011a) Contributions of ENSO and East Indian Ocean SSTA to the interannual variability of Northwest Pacific tropical cyclone frequency. *Journal of Climate*, 24, 509–521.
- Zhan, R., Wang, Y. & Tao, L. (2014) Intensified impact of East Indian Ocean SST anomaly on tropical cyclone genesis frequency over the western North Pacific. *Journal of Climate*, 27, 8724–8739.
- Zhan, R., Wang, Y. & Wu, C. (2011b) Impact of SSTA in the East Indian Ocean on the frequency of Northwest Pacific tropical cyclones: a regional atmospheric model study. *Journal of Climate*, 24, 6227–6242.
- Zhang, H., Wu, L., Huang, R., Chen, J.-M. & Feng, T. (2020) Does the Pacific meridional mode dominantly affect tropical cyclone genesis in the western North Pacific? *Climate Dynamics*, 55, 3469–3483.
- Zhang, W., Leung, Y. & Fraedrich, K. (2015) Different El Niño types and intense typhoons in the western North Pacific. *Climate Dynamics*, 44, 2965–2977.
- Zhang, W., Vecchi, G.A., Murakami, H., Villarini, G. & Jia, L. (2016) The Pacific meridional mode and the occurrence of tropical cyclones in the western North Pacific. *Journal of Climate*, 29, 381–398.
- Zheng, J., Wu, Q., Guo, Y. & Zhao, S. (2016) The impact of summertime North Indian Ocean SST on tropical cyclone genesis over the western North Pacific. *Scientific Online Letters on the Atmosphere*, 12, 242–246.

How to cite this article: Song, J., Klotzbach, P. J., Qin, N., & Duan, Y. (2024). Independent contributions of tropical sea surface temperature modes to the interannual variability of western North Pacific tropical cyclone frequency. *International Journal of Climatology*, 44(6), 1867–1882. <https://doi.org/10.1002/joc.8417>